scattering, flux peaking, etc.) can be built.

We wish to acknowledge helpful discussions with J. Bøttiger and W. L. Brown, and experimental assistance from R. Levesque. The thin gold crystal used in the measurements was kindly supplied by P. Ambrosius-Olson of Aarhus University.

*Work supported in part by a U. S. Atomic Energy Commission Graduate Fellowship.

[1]H. O. Lutz, S. Datz, C. D. Moak, and T. S. Noggle, Phys. Rev. Lett. 17, 6 (1966).

[2]W. M. Gibson, J. B. Rasmussen, P. Ambrosius-Olsen, and C. J. Andreen, Can. J. Phys. 46, 551 (1968).

[3]S. Datz, C. D. Moak, T. S. Noggle, B. R. Appleton, and H. O. Lutz, Phys. Rev. 179, 315 (1969).

[4]M. T. Robinson, Phys. Rev. 179, 327 (1969).

[5]B. R. Appleton, S. Datz, C. D. Moak, and M. T. Robinson, Phys. Rev. B 4, 1452 (1971).

[6]F. H. Eisen and M. T. Robinson, Phys. Rev. B 4, 1457 (1971).

[7]M. T. Robinson, Phys. Rev. B 4, 1461 (1971).

[8]C. Erginsoy, Phys. Rev. Lett. 15, 360 (1965).

[9]J. Lindhard, Kgl. Dan. Vidensk. Selsk., Mat.-Fys. Medd. 34, No. 14 (1965).

[10]L. D. Landau and E. M. Lifshitz, *Mechanics* (Pergamon, New York, 1960), p. 27.

[11]W. M. Gibson and J. Golovchenko, to be published.

[12]L. M. Milne-Thompson, in *Handbook of Mathematical Functions*, edited by M. Abramowitz and I. A. Stegun (U.S. GPO, Washington, D. C., 1964), p. 589.

Ultrasonic Spin Echoes

N. S. Shiren and T. G. Kazyaka
IBM Thomas J. Watson Research Center, Yorktown Heights, New York 10598
(Received 24 March 1972)

Generation and detection of ultrasonic spin echoes (phonon echoes) and of ultrasonically induced rf magnetic field spin echoes are reported. With the latter, signal-to-noise improvements of 2 orders of magnitude were found over direct ultrasonic absorption spectroscopy. The effects of momentum conservation selection rules are discussed, as are properties and applications of the various echoes.

We report the first observations of ultrasonic spin echoes (or phonon echoes), and of ultrasonically induced rf magnetic spin echoes. The ultrasonic spin echoes are generated following two-pulse sequences which consist of either two ultrasonic pulses (*UU* echo), or an ultrasonic pulse followed by an rf magnetic field pulse (*UH* echo). Ultrasonically induced rf spin echoes are generated by three-pulse sequences consisting of two ultrasonic pulses and an rf magnetic field pulse in any order (*UUH*, *UHU*, *HUU* echoes); these are stimulated echoes.[1] As discussed below, the form an echo takes (i.e., whether ultrasonic or magnetic), and its propagation direction, are determined by momentum conservation selection rules.[2] *UU* echoes are analogous to photon echoes,[3] and propagate in the forward direction (with respect to the ultrasonic pulses); *UH* echoes propagate in the backward direction. Ultrasonic spin echoes are of interest because their temporal decay measures the relaxation of off-diagonal components of magnetoelastic stress, whereas the decay of magnetic (*HH*) spin echoes[1] measures the relaxation of the off-diagonal magnetization. The relaxation time constants are not equal when the dominant spin-phonon coupling is quadratic in the spin operators, as is usual for non-Kramers ions. Therefore *UU* or *UH* echoes complement *HH* echoes in obtaining a complete description of paramagnetic relaxation processes. They should also be of use in the measurement of spin-phonon coupling constants. We believe the stimulated echoes can make ultrasonic paramagnetic resonance a more important adjunct to other EPR spectroscopic techniques than it has been heretofore, since we have observed signal-to-noise improvements of 2 orders of magnitude over direct ultrasonic absorption measurements on weakly coupled ions. In addition, they can be observed simultaneously with other EPR measurements in the same spectrometer.

The experiments were performed at 9 GHz on paramagnetic ions in concentrations $\approx 10^{-5}$ in MgO crystals at 1.8 and 4.2°K. The measurements reported here utilize 1.75-cm-long quartz transducers bonded to MgO crystals ≈ 1.25 cm in length, although our first observations were made using thin-film ZnO transducers deposited directly on the MgO. The ultrasonic measurements were of the reflection type; i.e., the generating cavity resonator (with the usual re-entrant configuration) also served as detector. rf magnetic field pulses were applied via a rectangular, dielectric filled, TE_{012} cavity resonator

with narrow dimension, ≈ 0.5 cm, parallel to the quartz-MgO axis (z axis), and located such that the bonded crystal faces lay just outside the entrance hole, in a geometry similar to one previously reported.[4] The rf magnetic field was oriented vertically (y axis). Magnetrons delivering 2 kW served as microwave sources for the ultrasonic pulses; 250 mW, from a pulse-modulated klystron, was sufficient for the rf magnetic field pulses. The frequencies of all pulses were the same, but phase coherence did not obtain among different inputs. The static Zeeman field, $\vec{H}_0$, could be rotated in the z-x plane. All measurements were made on $\Delta M = 1$ transitions with longitudinal ultrasonic waves propagating along z. The spin-phonon matrix element then varies as $\sin\theta\cos\theta$ (θ is the angle between $\vec{H}_0$ and $\hat{z}$), and in all measurements we have verified that the echo amplitudes peaked at $\theta = \frac{1}{4}\pi$ and vanished at $\theta = 0$ and $\frac{1}{2}\pi$.

UU echo.—This is the ultrasonic analog of the photon echo. The momentum conservation selection rule is,[3]

$$\vec{k}_e = 2\vec{k}_2 - \vec{k}_1, \qquad (1)$$

where e, 2, and 1 refer to the echo, second pulse, and first pulse, respectively. Since $\vec{k}_2 = \vec{k}_1$, the echo propagates in the same direction as the initial pulses. Figure 1 shows an echo generated by Ni^{2+}, as received in the ultrasonic cavity, for two different timings of the second pulse with respect to the first. The echo is formed during the round-trip traversal of the initiating pulses through the MgO. The very small amplitude of the echo is probably caused by absorption[5] ($\alpha \approx 5$ dB/cm) and by distortion of the initiating pulses by self-induced transparency.[6] This explanation is supported by the fact that we were unable to observe echoes on the more strongly absorbing $\Delta M = 2$ transition of Ni^{2+}. Observation of *UU* echoes should, therefore, be improved by making transmission measurements on thin samples, as in photon echo experiments. Ultrasonic spin echoes are generated by the precessing magnetoelastic stress. For this reason neither *UU* nor *UH* echoes were observable on the weakly coupled ions Fe^{3+}, and Mn^{2+}, which were also present in our crystals.[7]

UH echo.—The selection rule is again given by Eq. (1); however, in this case $|k_2| = 0$, therefore $\vec{k}_e = -\vec{k}_1$. The echo propagates in the reverse direction to the ultrasonic pulse. Its timing is such that it appears to be reflected from the front end of the active region (determined by the cavity dimension and/or bond location) at time $2t_2 - t_1$ (the usual echo formation time); t_2 is the onset time of the H pulse, and t_1 is the time at which the U pulse enters this region. Simple consideration of the retarded echo times at all points in the volume shows them to be equal for backward propagation, so that the echo amplitude is proportional to the volume integral. Because only one ultrasonic pulse is used, and because only a single traversal through the 0.5-cm active region is important for both it and the echo, rather than the full round-trip traversal of 2.5 cm, absorption and self-induced transparency are less important than for the *UU* echo. Thus in Fig. 2, the *UH* echoes are seen to be comparable in size to the ultrasonic pulses (compare Fig. 1). Various pulses are identified in Fig. 2, which shows the detected output of the ultrasonic cavity. The H pulse is observed by rf leakage. The origin of the time scale, marked 0 ($= t_1 \equiv 0$), is the time at which the U pulse (which is later detected at M_1) entered the active volume. (For this ex-

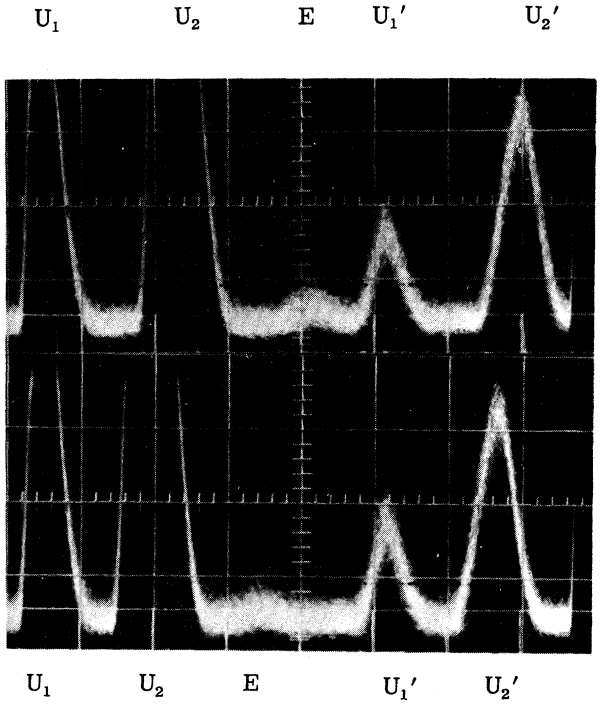

FIG. 1. Oscilloscope traces of output of ultrasonic cavity showing *UU* echoes, E, for two timings of the ultrasonic pulses, U_1 and U_2. U_1' and U_2' are second round-trip traversals in MgO. Ni^{2+} resonance field. 0.5 μ sec/div.

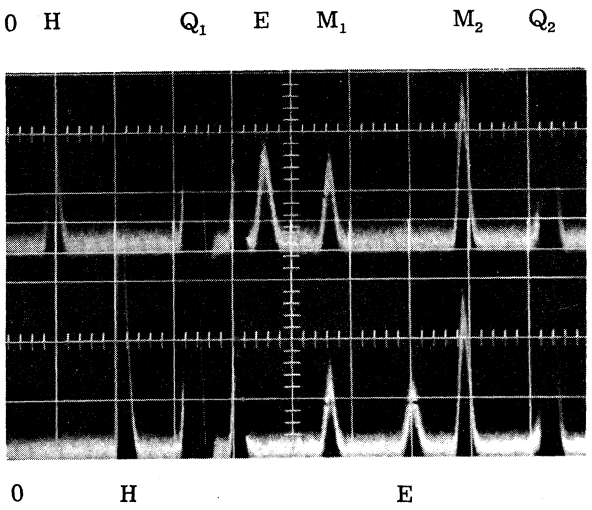

FIG. 2. Oscilloscope traces of output of ultrasonic cavity showing *UH* echoes, *E*, for two timings of the *H* pulse. *Q* and *M* refer to pulses in quartz and MgO (see text). A shear-wave pulse propagating only in the quartz has been blocked out. Ni^{2+} resonance field. 1 μsec/div.

periment this time was determined by the bond location.) Thus, *H* marks the time t_2; Q_1 marks a reflected pulse in the quartz and is thus the one-way traversal time in the quartz; Q_2 is a second round trip in the quartz; M_1 and M_2 are round trips in the MgO plus the traversal time, Q_1, to arrive at the detector; *E* is the echo time, $2t_2$, plus Q_1. The manifestation of the "reflected" echo is particularly noticeable on the upper trace of Fig. 2, where *E* appears before M_1.

The decay of *HH* echoes measures the relaxation of $\langle S_\pm \rangle$ [$= \mathrm{Tr}(\rho S_\pm)$; ρ is the density operator], while that of ultrasonic echoes measures the relaxation of $\langle S_\pm S_z + S_z S_\pm \rangle$. Earlier spin echo measurements[6] gave 1.2 μsec for the decay constant of *HH* echoes on Ni^{2+} in these samples at 1.8°K, and this measurement has been verified in the present work. We have not yet completed a detailed study of the *UH* echo decay but it is at least a factor of 3 slower, as may be seen by direct measurement in Fig. 2. A possible explanation is offered by the work of Smith, Dravnieks, and Wertz[8] who applied Redfield's relaxation theory to Ni^{2+} assuming direct relaxation to the lattice. Their results show that the dominant decay rate of $\langle S_+ S_z + S_z S_+ \rangle$ is smaller than that of $\langle S_\pm \rangle$. This result depends only upon the symmetry of the relaxation matrix. In our experiments at low temperatures, spin-lattice relaxation is too slow to explain the echo decays; the dominant off-diagonal relaxation process is probably through dipole-dipole coupling to ions, such as Fe^{2+}, which are more strongly coupled to the lattice. However, both the dipole-dipole and spin-lattice Hamiltonians form bases for the fivefold representation of $\mathfrak{D}_3$, so the relaxation theory has the same form for both interactions. Through the use of both *HH* and *UH* echoes, together with a measurement of T_3, it is possible to completely determine all three independent relaxation parameters specified in Ref. 8.

HUU, UHU, and UUH stimulated echoes.—These are rf echoes observed in the resonance cavity. The two ultrasonic pulses may be derived from separate sources, as in the case of *UU* echoes. However, it is simpler to use one initial pulse and take advantage of the many round-trip traversals in the host crystal, as well as those in the transducer which are partially transmitted when incident on the bond. Of the four possible three-pulse echoes discussed by Hahn,[1] only the stimulated echoes at $t_e = t_3 + t_2$ ($t_1 \equiv 0$) and $t_e = 2(t_3 - t_2)$ are allowed by the selection rules, and the latter only in the case *HUU* when both *U* pulses propagate in the same direction. The former is allowed in all cases, but for *HUU* the *U* pulses must propagate in opposite directions, while for *UHU* and *UUH* they must propagate in the same direction. The selection rules for these echoes are, respectively,

$$\vec{k}_e = \vec{k}_3 + \vec{k}_2 - \vec{k}_1, \tag{2}$$

$$\vec{k}_e = 2(\vec{k}_3 - \vec{k}_2) + \vec{k}_1. \tag{3}$$

For an rf echo $|k_e| = 0$; $|k_1|$, $|k_2|$, or $|k_3|$ is zero for *HUU*, *UHU*, or *UUH*, respectively. We were unable to observe echoes obeying Eq. (3); however, those governed by Eq. (2) were seen for many allowed combinations of traversals. The following discussion refers to the echo generated with two *U* pulses formed from two successive passes in the MgO.

Because the rf echo, even though ultrasonically induced, is generated by the precessing magnetization rather than magnetoelastic stress, it can be observed on ions with very weak spin-phonon couplings. It is, of course, necessary that the ultrasonic pulses have sufficient power to drive the spin system, but this is generally not a restriction. In Fig. 3 we show spectra of Fe^{3+} and Mn^{2+} in MgO, taken by *UUH* echoes and by ultrasonic absorption. The signal-to-noise improvement is about 100:1 on the Fe^{3+}, and greater on the Mn^{2+} which cannot be seen at all in the absorp-

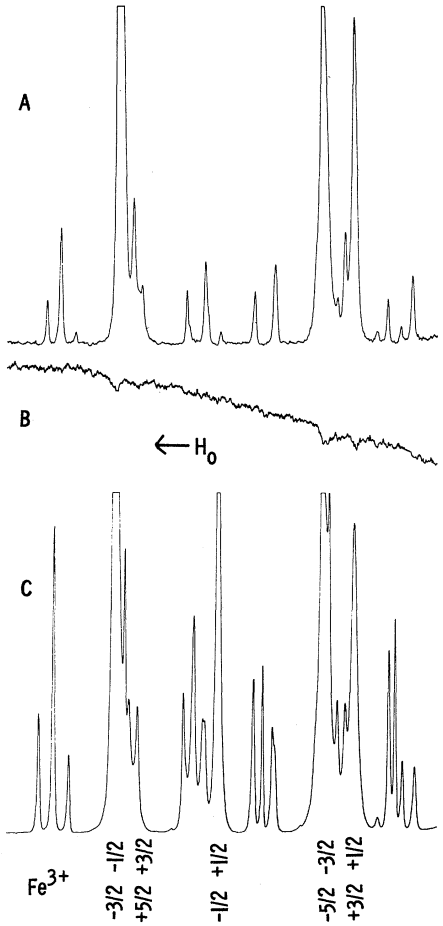

FIG. 3. Fe^{3+} and Mn^{2+} spectra in MgO (*not* an artist's tracing), taken by (a) *UUH* echoes, (b) ultrasonic absorption, and (c) *HH* echoes. H_0 approximately parallel to ⟨101⟩. Fe^{3+} transitions are labeled; Mn^{2+} similar but only the lowest-field hyperfine group is fully split. For a complete description of the spectra see Ref. 9.

tion spectrum. A spectrum taken with *HH* echoes is also shown. Note that the central $(+\frac{1}{2}, -\frac{1}{2})$ transitions of Mn^{2+} are missing in the *UUH* spectrum, as dictated by quadrupolar spin selection rules. It is present, but small, in the Fe^{3+} spectrum because with H_0 parallel to ⟨101⟩ there is a small admixture of other spin states. This illustrates how simultaneous measurements by both echo techniques complement each other in the identification of spectra.

We are investigating the possibility of observing stimulated echoes on $\Delta M = 2$ transitions by methods similar to the Raman echoes discussed by Hartmann.[10]

We wish to acknowledge discussions with Dr. G. Burns and Dr. D. Grischkowsky.

[1]E. L. Hahn, Phys. Rev. 77, 297 (1950).
[2]These rules may be easily deduced by expressing the times at which echoes form (as given, e.g., in Ref. 1) in terms of the retarded times of the pulses.
[3]I. D. Abella, N. A. Kurnit, and S. R. Hartmann, Phys. Rev. 141, 391 (1966).
[4]N. S. Shiren, Phys. Rev. Lett. 11, 3 (1963).
[5]E. L. Hahn, N. S. Shiren, and S. McCall, Phys. Lett. 37A, 265 (1971).
[6]N. S. Shiren, Phys. Rev. B 2, 2471 (1970).
[7]The spin phonon coupling constants, G_{11}, are (in units of cm^{-1}/unit strain) Ni^{2+}, 57; Fe^{3+}, 5; Mn^{2+}, 1.4. See G. D. Watkins and E. Feher, Bull. Amer. Phys. Soc. 7, 29 (1962); N. S. Shiren, Bull. Amer. Phys. Soc. 7, 29 (1962).
[8]S. R. P. Smith, F. Dravnieks, and J. E. Wertz, Phys. Rev. 178, 471 (1969), Eq. (24).
[9]W. J. Low, *Paramagnetic Resonance in Solids* (Academic, New York, 1960).
[10]S. R. Hartmann, IEEE J. Quantum Electron. 4, 802 (1968).

Hyperchanneling, an Axial Channeling Phenomenon*

B. R. Appleton, C. D. Moak, T. S. Noggle, and J. H. Barrett
Oak Ridge National Laboratory, Oak Ridge, Tennessee 37830
(Received 31 January 1972)

We have studied the behavior of 21.6-MeV I ions undergoing proper axial channeling (hyperchanneling) in Ag. Ions of this special class traverse the crystal within a single axial channel and as a result exhibit conspicuously lower energy losses and an order of magnitude smaller acceptance angles than ordinary axially channeled ions. Analysis of the results indicates that hyperchanneled ions provide a new means for studying multiple scattering radiation damage, and ion-atom potentials in solids.

Detailed studies of the energy loss of 21.6-MeV I ions axially channeled in Ag single crystals show that over a small range of incidence angles with respect to [011] a distinct group of channeled ions exhibits unusually low energy losses. We identify this group as ions which remain within

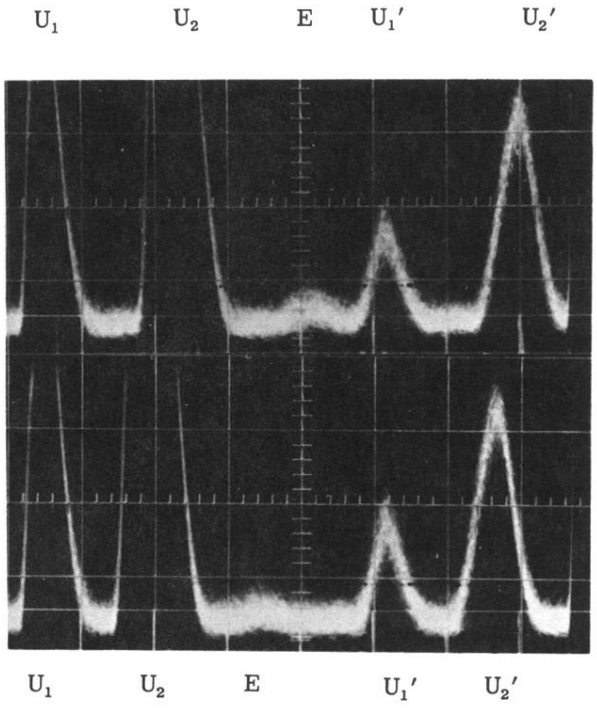

FIG. 1. Oscilloscope traces of output of ultrasonic cavity showing *UU* echoes, *E*, for two timings of the ultrasonic pulses, U_1 and U_2. U_1' and U_2' are second round-trip traversals in MgO. Ni^{2+} resonance field. 0.5 μ sec/div.

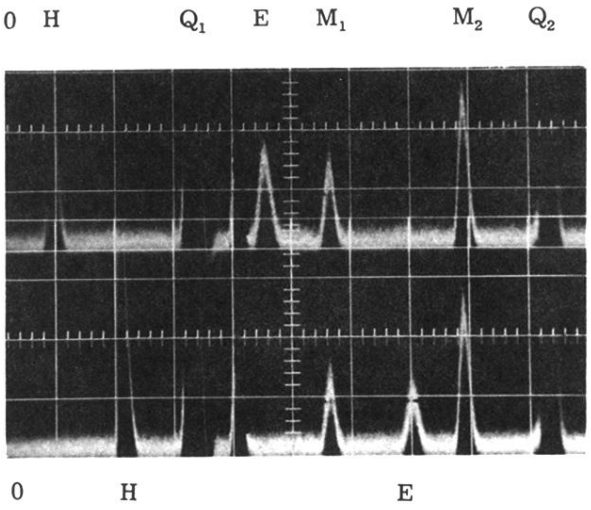

FIG. 2. Oscilloscope traces of output of ultrasonic cavity showing *UH* echoes, *E*, for two timings of the *H* pulse. *Q* and *M* refer to pulses in quartz and MgO (see text). A shear-wave pulse propagating only in the quartz has been blocked out. Ni^{2+} resonance field. 1 μ sec/div.